European Journal of Pharmaceutical Sciences 174 (2022) 106200

Contents lists available at ScienceDirect

European Journal of Pharmaceutical Sciences

journal homepage: www.elsevier.com/locate/ejps

Spray-dried indomethacin-loaded polymeric micelles for the improvement of intestinal drug release and permeability

Bence Sipos [a], Ildikó Csóka [a], Rita Ambrus [a], Zsuzsanna Schelz [b], István Zupkó [b], György Tibor Balogh [b,c], Gábor Katona [a,*]

[a] Faculty of Pharmacy, Institute of Pharmaceutical Technology and Regulatory Affairs, University of Szeged, Eötvös str. 6, Szeged H-6720, Hungary
[b] Department of Pharmacodynamics and Biopharmacy, Faculty of Pharmacy, University of Szeged, Eötvös str. 6, Szeged H-6720, Hungary
[c] Department of Chemical and Environmental Process Engineering, Budapest University of Technology and Economics, Műegyetem quay 3, Budapest H-1111, Hungary

ARTICLE INFO

Keywords:
Polymeric micelle
Spray-drying
Indomethacin
Solubility enhancement
Oral delivery

ABSTRACT

Current study aimed to develop a spray-dried powder containing indomethacin (IND)-loaded polymeric micelles which can be administered perorally as a dissolved powder to enhance the drug release and permeability of the active substance. The resulting low dense spray-dried spherical particles have decreased particle size (7.21 μm) in monodisperse distribution. The polymeric micelles had a nano size range (130 nm) also in monodisperse size distribution. These nanoparticulate properties and the high encapsulation efficiency (> 80%) lead to the improvement of gastrointestinal drug release in fasted and fed state conditions. Following second order and Higuchi kinetics, a rapid drug release was experienced exceeding the initial IND suspension. *In vitro* cell line studies on Caco-2 human colorectal adenocarcinoma cells showed that the formulation does not increase the toxicity of initial IND, therefore can be considered safe for oral application. *Ex vivo* semiquantitative and quantitative studies were performed on porcine small intestine where increased flux and permeability values of IND were achieved. The physical stability of the solid formulation was sufficient through a 6-month intermediate study caused by the hydrogen-bond formation between IND and the micelle-forming co-polymer.

1. Introduction

Oral drug delivery is a popular and the most common way of administering active pharmaceutical ingredients (APIs). Nowadays, however, increasing patient demands, a significant deterioration in therapeutic progressions and alternatives, and changing industry expectations call for the production of innovative formulations that meet the newly-expected demands (Mohammed et al., 2019). The current dosage forms for peroral use also include the problem of not sufficient drug release, drug permeation across intestinal barriers. This also leads for the need of (a) finding the proper formulation process for increased stability; (b) utilizing nanomedical formulations for improving bioavailability.

Spray-drying is a common and industrially acceptable product development method offering various advantageous properties of the final drug formulation (Party et al., 2021). As an alternative to freeze-drying, it is a technique with higher scalability with proper control of the particle characteristics of the final solid product (Ruphuy et al., 2020; Eun et al., 2020). Spray-drying is acceptable to utilize in the development of dosages forms containing small molecules for oral delivery, as the end product can be formulated into a rapidly dissoluble solid product due to the increased flowability and wettability properties (Baumann et al., 2021). Spray drying is advantageous as it is an attractive technology to produce microparticles, in which nanoparticle forming materials can be encapsulated with a rapid, single-step operational drying. Number of studies have also demonstrated that besides the high temperature operation, labile (nano)therapeutics can be formulated by this method (Bowey and Neufeld, 2010; Yan et al., 2011). The high solubility and rapid dissolution kinetics can be exploited through oral delivery, where according to the general biopharmaceutical model, drug release also promotes faster and higher levels of gastrointestinal permeation (Eleraky et al., 2020; Wijiani et al., 2020).

Rapid carrier dissolution is of paramount importance in case of the polymeric micelles as well, where the general main goal is to not hinder the advantageous solubilizing, drug release and permeation enhancing effects of the applied polymers. Polymeric micelles consist of surfactant-

* Corresponding author.
E-mail address: katona.gabor@szte.hu (G. Katona).

https://doi.org/10.1016/j.ejps.2022.106200
Received 3 February 2022; Received in revised form 28 April 2022; Accepted 29 April 2022
Available online 1 May 2022

Table 1
Composition of the feeding solution containing the IND-loaded polymeric micelles.

Component	Amount
Indomethacin (mg/ml)	0.625
Soluplus (mg/ml)	7.5
D-trehalose dihydrate (% w/v)	5
Tween 80 (% w/v)	0.50

like amphiphilic graft co-polymers which co-polymers can self-assemble into nanocarriers above the critical micellar concentration (CMC) and -temperature (CMT) (Yokoyama, 2010; Deshmukh et al., 2017). In contrast to classic surface-active solubilizers they offer higher circulation time, dilution and physical stability, increased drug loading and water solubility (Sipos et al., 2021). Generally speaking, many transport mechanisms take place in their absorption through the gastrointestinal tract including active and passive transport, endocytosis and facilitated transport routes as well (Gaucher et al., 2010). Soluplus® (SP, polyvinyl caprolactam-polyvinyl acetate-polyethylene glycol graft copolymer (PCL-PVAc-PEG)) is a commonly applied co-polymer to formulate solid dispersions via melt technology or polymeric micelle development (Sipos et al., 2020). Micelle formation of SP is a novel approach to enhance bioavailability of poorly water-soluble drugs. SP forms approximately 80 nm-in-size polymeric micelles by itself above a very low critical micellar concentration of 7.6 mg/ml (Alvarez-Rivera et al., 2016; Rahman et al., 2020). It is highly tolerable by the human body with low toxicity (the oral and dermal median lethal dose values for human (lethal dose, 50%; LD_{50}) are both >5 g/kg), especially through peroral administration. The main strength of this co-polymer lies in the following: low CMC value, high circulation stability, small protein-mediated polymer degradation tendency along with high solubilization capacity (Simões et al., 2015; Xia et al., 2016). Their problem in liquid dosage form is the short-term stability, for which the solution can be the following: the product should be placed on market in a solid powder form, which will be later dispersed in water before the first use by the patient or the medical staff. This will decrease the chance for the particle aggregation, cluster formation or active substance precipitation.

Perorally administered drugs usually have low bioavailability due to degradation mechanisms caused by the changing pH conditions of the gastrointestinal tract and the hepatic metabolic enzymes, poor water solubility and permeability through endothelial barriers. Indomethacin (IND) is a common example of this along with many non-steroidal anti-inflammatory drugs (NSAID). This results in higher dosages to be administered to the patients causing increased side-effect profile, especially gastrointestinal ulcers. As it is a commonly applied NSAID in arthritis and gout, it can be claimed that mostly elderly patients are medicated with this drug, which geriatric differences also contribute to the poor patient adherence due to increased side effects and insufficient therapeutic response (Badri et al., 2016; Irvine et al., 2018).

There is an increased need for the value-added pharmaceutical products, which led to our aim to develop a stable sugar-alcohol based carrier system, homogenously containing a polymeric micelle formulation via spray-drying. Spray-drying was carried out to achieve a rapidly dissolving dry powder which can be administered perorally via dissolving the end product in water and drinking it. The powder and micelle characteristics were evaluated in order to describe the background of the solubility augmentation mediated drug release enhancement. Our hypothesis was that by utilizing the rapid, one-step operation of spray-drying, a proper polymeric micelle-based nanomedical formulation can be achieved with the above-mentioned advantages. By increasing the water solubility of a Biopharmaceutical Classification System (BCS) Class II drug, a more efficient, rapid permeation can be achieved utilizing this nanotechnological approach.

2. Materials and methods

2.1. Materials

The micelle-forming agent Soluplus® (SP, polyvinyl caprolactam-polyvinyl acetate-polyethylene glycol graft copolymer (PCL-PVAc-PEG)) was provided from BASF GmbH (Hanover, Germany). Indomethacin (IND), D-trehalose-dihydrate (D-Tre), Tween 80, phosphate buffer saline (PBS) powder, sodium acetate and acetic acid were purchased from Merck Ltd. (Budapest, Hungary). Analytical grade solvents methanol, acetonitrile and cholesterol (CHO), L-α-phosphatidylcholine (PC) were also obtained from Merck Ltd. Powders for the biorelevant gastric and intestinal fluids were purchased from Biorelevant.com Ltd. (London, United Kingdom). Distilled water was purified for the experiments using the Millipore Milli-Q® Gradient Water Purification System (Merck Ltd., Budapest, Hungary).

2.2. Formulation process of IND-loaded polymeric micelles

The formulation of spray-dried IND-loaded polymeric micelles were performed in two steps. At first, 50 ml of aqueous SP (15 mg/ml) and 50 ml of ethanolic IND (1.25 mg/ml) solutions were prepared. The polymer solution was placed on a magnetic stirrer and the IND solution was added dropwise to it at a rate of 0.5 ml/min. The system was kept under constant stirring (250 rpm) for 2 h at 25°C, then D-trehalose dihydrate (5% w/v) and Tween 80 (0.25% w/v) was dissolved. The total volume of the ethanolic-aqueous solution was 100 ml. The composition of the feeding solution is presented in Table 1.

The solid formulation was produced by spray-drying using a spray-dryer equipped with a two-fluid nozzle with 0.7 mm nozzle tip diameter (Büchi Mini Spray Dryer B-191, Büchi, Flawil, Switzerland). The spray drying properties were the following: inlet temperature: 110°C, outlet temperature: 80°C, aspirator capacity: 80%, airflow rate: 500 l/h and feed pump rate: 5%. The average yield was 78.4 ± 1.2%.

A 7-factor, 8-run Plackett-Burman factorial design was performed where the composition and the spray-drying settings varied. The runs were evaluated by average particle size (D[0.5]) and distribution (Span) and by the micelle characteristics (average hydrodynamic average and polydispersity index (PdI)). Run. No. 7 fitted the criteria of our goals, therefore that formulation was further investigated (referred as IND-PM). The factorial design with the corresponding measured values can be found in the Tables 2 and 3.

2.3. Quantitative measurement of IND via HPLC

The determination of IND concentration was performed with high performance liquid chromatography (HPLC) using an Agilent 1260 Infinity (Agilent Technologies, Santa Clara, CA, USA) instrument. The stationary phase was a Kinetex® EVO C18 LC column (50 μm, 110 Å, 150 mm x 4.6 mm) (Phenomenex, Torrance, CA, USA). The mobile phases were pH 5.0 0.05 M acetate buffer (A) and acetonitrile (B) applied in 40:60 ratio. The separation was performed by isocratic elution for 5 min at 40°C with a flow rate of 1 ml/min. The volume of aliquots was 10 μl. Chromatograms were detected at 254 nm using UV-Vis diode array detector. The chromatograms were evaluated using ChemStation B.04.03. Software (Agilent Technologies, Santa Clara, CA, USA). The retention time of IND was at 2.25 min. The limit of detection (LOD) and limit of quantification (LOQ) of IND were 15.69 and 47.56 ppm, respectively. The calibration was performed from 1 to 10 μg/ml and from 0.1 to 1.0 mg/ml of IND, where the determination coefficients of linearity (R^2) were 0.9991 and 0.9996, respectively.

2.4. Characterization of IND-loaded spray-dried polymeric micelles

2.4.1. Determination of particle size and distribution

In order to determine the particle size and particle size distribution of

Table 2
Plackett-Burman factorial design of the development of IND-loaded spray-dried polymeric micelles.

Run No.	IND [mg/ml]	SP [mg/ml]	Tween 80 [% w/v]	D-tre [% w/v]	Inlet temperature [°C]	Aspirator capacity (%)	Feed pump rate [%]
PB1	1.25	7.5	0.25	10	120	80	5
PB2	1.25	15	0.25	5	110	70	5
PB3	1.25	15	0.50	5	120	80	3
PB4	0.625	15	0.50	10	120	70	5
PB5	1.25	7.5	0.50	10	110	70	3
PB6	0.625	15	0.25	10	110	80	3
PB7	0.625	7.5	0.50	5	110	80	5
PB8	0.625	7.5	0.25	5	120	70	3

Table 3
D[0.5] and Span values from the laser diffraction measurement of the spray-dried particles. Z-average and PdI values from the dynamic light scattering measurements obtained after in-water dispersion of the spray-dried particles. The 8-run Plackett Burman design was measured in order to find the optimized polymeric micelle formulation. Data are presented as means ± SD ($n = 3$).

Run No.	D [0.5] (μm)	Span	Z-average (nm)	PdI
PB1	33.666 ± 8.14	5.159 ± 0.256	493.1 ± 53.1	0.491 ± 0.019
PB2	13.121 ±2.47	2.692 ± 0.165	143.4 ± 12.7	0.221 ± 0.023
PB3	9.003 ± 3.15	3.369 ± 0.199	139.7 ± 3.9	0.265 ± 0.041
PB4	8.294 ±1.58	4.849 ± 0.360	105.4 ± 5.8	0.250 ± 0.008
PB5	6.859 ± 0.98	1.768 ± 0.412	202.1 ± 17.6	0.406 ± 0.074
PB6	5.793 ± 1.05	4.444 ± 0.398	94.9 ± 6.4	0.182 ± 0.039
PB7	7.207 ± 0.36	1.789 ± 0.097	130 ± 2.3	0.241 ± 0.007
PB8	5.82 ± 1.27	2.299 ± 0.084	127.5 ± 11.3	0.236 ± 0.011

the spray-dried formulation, laser diffraction was used (Malvern Mastersizer Scirocco 2000, Malvern Instruments Ltd., Worcestershire, UK). The dry dispersion unit was used to measure the spray-dried formulation. Approximately 0.3–0.5 g of product was loaded into the feeding tray. The dispersion air pressure was adjusted to 3.0 bar and a vibration feed of 75% was used. All measurements were carried out in triplicate. The particle size distribution was characterized by the D[0.1] – 10% of the volume distribution is below this value; D[0.5] – the volume median diameter; D[0.9] – 90% of the volume distribution is below this value, D [3,2] – Sauter mean diameter; D[4,3] – De Brouckere mean diameter and the calculated Span (as the width of the distribution) values. Span was calculated via the following equation:

$$\text{Span} = \frac{D[0.9] - D[0.1]}{D[0.5]} \quad (1)$$

2.4.2. Morphological investigation

To characterize the morphology of the spray-dried formulation, scanning electron microscopy (SEM) (Hitachi S4700, Hitachi Scientific Ltd., Tokyo, Japan) was used. A high voltage of 10 kV, an amperage of 10 mA and an air pressure of 1.3–13.1 mPa was applied. A high vacuum evaporator and argon atmosphere were used to form the sputter-coated samples conductive with gold-palladium (Bio-Rad SC 502, VG Microtech, Uckfield, UK). The thickness of the gold-palladium coating was approximately 10 nm.

2.4.3. Density measurement

Bulk and tapped densities of the spray-dried formulation were measured using an Engelsmann Stampfvolumeter (Ludwigshafen, Germany). A 10 cm^3 cylinder was filled with 10 cm^3 of powder to calculate bulk density. Then, it was tapped 1500 times. The tapped density was calculated compared with the volume prior and following the taps. All measurements were carried out in triplicate. The following flow characters were calculated using Eqs. (2) and (3):

$$\text{Hausner ratio} = \frac{\rho_t}{\rho_b} \quad (2)$$

$$\text{Carr index} = \frac{\rho_t - \rho_b}{\rho_b} \times 100 \quad (3)$$

where ρ_t is the tapped density and ρ_b is the bulk density.

2.4.4. Drug content

The drug content of spray-dried formulations was measured via HPLC. 100 – 200 mg of the samples were weighed, then dissolved in 2 ml of methanol – purified water mixture (50 – 50 ratio) and the solutions were measured via the HPLC method described before. The IND amount was expressed as the percentage of the weighed spray-dried formulation. The measurements were carried out in triplicate, data is presented as means ±SD.

2.4.5. Dynamic light scattering and zeta potential measurements

For the determination of the average hydrodynamic diameter (expressed as Z-average), polydispersity index (PdI) and zeta potential, the spray-dried particles were dissolved in water to achieve in-water dispersed IND-loaded polymeric micelles and dynamic light scattering (DLS) was used via a Malvern Zetasizer Nano ZS (Malvern Instruments, Malvern, UK) equipment. The measurement conditions were the following: the temperature was set at 25°C, the refractive index of IND was 1.680 and the measurements took place in folded capillary cells. All measurements were carried out in triplicate, data is presented as means ±SD.

2.4.6. Determination of thermodynamic solubility and encapsulation efficiency

In order to quantify the increase in the water solubility of IND in the micellar system, the thermodynamic solubility was measured. 0.5 ml of purified water was measured into vials and the formulation was dissolved until visible saturation. Covered with parafilm, the saturated solution was under constant stirring on a magnetic stirrer for 72 h at ambient temperature. Then, the solutions were filtered with a 0.22 μm pore-sized polyethersulfone (PES) membrane. The passed through IND concentration was measured via HPLC, as it contains the IND amount which is either in dissolved form or entrapped in the micellar core making up the effective dissolved concentration. All measurements were carried out in triplicate (Sipos et al., 2020; Sipos et al., 2021).

In order to determine the encapsulation efficiency of the spray-dried micelles, the indirect method was chosen. The IND-loaded micelles were separated from the aqueous media via centrifugation using a Hermle Z323 K high performance refrigerated centrifuge (Hermle AG, Gosheim, Germany) at 13,500 rpm, 25°C for 30 min. The clear supernatant was diluted 5-fold with methanol, then the quantitative measurements were carried out via HPLC. All measurements were carried out in triplicate. The encapsulation efficiency (EE%) was calculated via Eq. (4):

$$EE\% = \frac{\text{initial IND (mg)} - \text{measured IND (mg)}}{\text{initial IND (mg)}} \times 100 \quad (4)$$

2.4.7. Investigation of wettability and polarity

OCA Contact Angle System (Dataphysics OCA 20, Dataphysics Inc., GmbH, Germany) was used to determine the surface free energy and

polarity of the spray-dried polymeric micelles and its components. 0.15 g of spray-dried product was compressed by a Specac® hydraulic press (Specac Inc., USA) under 1 ton of pressing force. The contact angles of the pressings were determined as liquid mediums were dropped onto the surface of these pressings. Two liquid mediums were used for the measurements: 4.3 µl polar bidistilled water (interfacial tension of polar component (γ_i^p) = 50.2 mN/m, interfacial tension of disperse component (γ_i^d) = 22.6 mN/m) and 4.3 µl apolar diiodomethane (γ_i^p =1.8 mN/m, γ_i^d =49 mN/m). The solid surface free energy is derivable from the sum of the polar (γ_i^p) and non-polar (γ_i^d) components and was calculated according to the Wu equation (Radacsi et al., 2019):

$$(1+\cos\Theta)\gamma_l = \frac{4\left(\gamma_s^d\gamma_l^d\right)}{\gamma_s^d\gamma_l^d} + \frac{4\left(\gamma_s^p\gamma_l^p\right)}{\gamma_s^p\gamma_l^p} \quad (5)$$

where Θ is the contact angle, γ_s is the solid surface free energy and γ_l is the liquid surface tension. The percentage polarity was calculated as the percentage of the quotient of the γ_p and γ values (Eq. (6)).

$$\text{Polarity } (\%) = \frac{\gamma_p}{\gamma} \times 100 \quad (6)$$

2.5. Structure investigations

2.5.1. X-ray powder diffraction

The crystallinity of the spray-dried polymeric micelles was characterized by X-ray powder diffraction (XRPD) using a Bruker D8 Advance X-ray diffractometer (Bruker AXS GmbH, Karlsruhe, Germany) with Cu K λI radiation (λ = 1.5406 Å) and a VANTEC-1 detector. 40 kV of voltage and 40 mA of amperage were used during the measurements. The angular range was 3° to 4° 2θ with a step time of 0.1 s and a step size of 0.007°. The manipulations and evaluations were carried out using the EVA Software.

2.5.2. Thermoanalytical measurements

Differential scanning calorimetry (DSC) examinations were carried out using a Mettler-Toledo 821e DSC (Mettler-Toledo GmbH, Gießen, Germany) at the temperature interval of 25 to 300°C with the heating rate of 10°C/min under a constant argon flow of 150 ml/min. For the measurements, 5 ± 0.3 mg of the samples were placed in 40 µl aluminium pans. Each measurement was normalized to sample size.

2.5.3. Raman spectroscopy

To investigate the polymeric micelles via Raman spectroscopy, a Thermo Fisher DXR Dispersive Raman Instrument (Thermo Fisher Scientific, Inc., Waltham, MA, USA) equipped with a CCD camera and a diode laser (780 nm) was used. Raman measurements were carried out with a laser power of 24 mW at 50 µm split aperture size with an exposure time of 4 s and acquisition time of 6 s, for a total of 32 scans per spectrum in the spectral range of 3500 to 200 1/cm with cosmic ray and fluorescence corrections. To investigate the distribution of IND in the spray dried formulation, pastilles were formed using a Specac® hydraulic press (Specac Inc., USA) under 1 ton of pressing force. The distribution of IND was investigated by Raman chemical mapping. A 100 µm x 100 µm size surface was analysed with a step size of 10 µm, exposure time of 4 s and acquisition time of 6 s, for a total of 32 scans per spectrum. The Raman spectra were normalized in order to eliminate the deviation of intensity between the measured areas.

2.6. Physical stability study

The physical stability investigation was conducted accordingly to the ICH Q1A(R2) Stability Testing of new Drug Substances and Products guideline (ICH Q1A(R2), 2003). The intermediate study was performed where the spray-dried samples were stored at 30 ± 2°C and 65 ± 5% relative humidity (RH). At predetermined points: 0, 1, 3 and 6 months, the dry product was measured via laser diffraction and another portion was dissolved in purified water, then dynamic light scattering and zeta potential measurements took place. All measurements were carried out in triplicate, data is presented as means ±SD.

2.7. In vitro drug release study

A two-stage biorelevant drug release test was used to determine the drug release kinetics of the spray-dried formulations (Wang et al., 2009; Uhljar et al., 2021). The modified paddle method (Hanson Research SR8-Plus Dissolution Test Station, Chatsworth, CA, USA) was used to measure the drug release. The paddle was rotated at 100 rpm, the temperature was set at 37.5°C and the volume of the dissolution media was 200 ml. The formulations were dissolved in purified water and the amount of IND placed in dialysis bags (Spectra/Por® Dialysis Membrane with a MWCO value of 12–14 kD (Spectrum Laboratories Inc., Rancho Dominguez, CA, USA)) was chosen to be 25 mg, based on the drug content. For the first 30 min of the study, the dialysis bags were placed in Fasted State Simulated Gastric Fluid (FaSSGF) or Fed State Simulated Gastric Fluid (FeSSGF), then immediately these bags were transferred into Fasted State Simulated Intestinal Fluid (FaSSIF) or Fed State Simulated Intestinal Fluid (FeSSIF) where the sampling was continued up to 120 min. The sampling was performed at predetermined time points: 5, 15, 30, 45, 60 and 120 min. 1 ml was taken each time as aliquots for quantification via HPLC. Each experiment was performed in triplicate, data is presented as means ±SD. As a reference, IND suspension was used which was suspended by 0.025%w/w of hyaluronic acid to keep the particles stably suspended.

2.8. Modelling the in vitro kinetics

The release kinetics of IND from the polymeric micelle formulation was compared with the release kinetics of the initial IND. Six different mathematical models (zero order, first order, second order, Hixson-Crowell, Higuchi and Korsmeyer-Peppas model) were fitted with the obtained cumulative drug release vs. time curves to describe the kinetics and half-time, rate constants and regression coefficient values were calculated (R^2) To evaluate which model was followed, the values of the regression coefficient were determined and compared (Gouda et al., 2017; Wójcik-Pastuszka et al., 2019).

2.9. Rapid equilibrium dialysis measurement

To investigate the equilibrium kinetics of the dispersed spray-dried formulations, the Rapid Equilibrium Dialysis (RED) Device (Thermo Scientific™, Waltham, MA, USA) was used. The initial IND and the polymeric micelle formulation dispersed in pH 6.5 PBS was placed in the donor phase. To the dialysis, at first, RED inserts (8K MWCO) were fitted into the PTFE base plate, then 150 µl of the samples were placed into the donor chambers. Then, 300 µl of PBS (pH 6.5) was added to the acceptor chambers, and the unit was covered with a sealing tape and incubated at 37°C on an orbital shaker (350 rpm) for 6 h. 50 µl samples were withdrawn at predetermined time intervals (5, 15, 30, 60, 120, 240 and 360 min) from the acceptor chambers and immediately replaced with fresh PBS. IND concentration was measured using HPLC. Five parallel measurements were performed.

2.10. PAMPA permeability assay

Intestinal parallel artificial membrane permeability assay (PAMPA-Int) was applied to determine the effective Int-specific permeability of IND from the spray-dried formulation. The donor solutions were the formulation and the initial IND dispersed in pH 6.5 PBS. The filter donor plate (Multiscreen™-IP, MAIPN4510, pore size 0.45 µm; Millipore) was coated with 5 µl of lipid solution (16 mg PC + 8 mg CHO dissolved in 600 µL dodecane). Then the donor plate was fitted into the acceptor plate (Multiscreen Acceptor Plate, MSSACCEPTOR; Millipore) containing 300

Table 4
Laser diffraction measured particle size parameters of initial IND and the spray-dried IND-PM formulation. Data are presented as means ± SD ($n = 3$).

	IND	IND-PM
D[0.1] (μm)	9.67 ± 0.41	2.33 ± 0.11
D[0.5] (μm)	33.61 ± 1.24	7.21 ± 0.36
D[0.9] (μm)	183.3 ± 13.5	15.23 ± 1.02
Span	5.166 ± 0.457	1.789 ± 0.097
D[3.2] (μm)	15.37 ± 1.10	3.82 ± 0.21
D[4.3] (μm)	72.56 ± 4.89	7.24 ± 0.56

μl of PBS solution (pH = 7.4), and 150–150 μl of the donor solutions were put on the membrane of the donor plate. The donor plate was covered with a sheet of wet tissue paper and a plate lid to avoid evaporation of the solvent. The sandwich system was incubated at 37°C for 4 h (Heidolph Titramax 1000), followed by separation of the PAMPA sandwich plates and the determination of concentrations of IND in the acceptor solutions by HPLC. Six parallel measurements took place. The effective permeability and membrane retention of drugs were calculated using the following equation (Avdeef, 2012):

$$P_e = -\left(\frac{2.303 \times V_A}{A(t - \tau_{SS})}\right) \times \log\left[1 - \frac{c_A(t)}{s}\right] \quad (7)$$

where P_e is the effective permeability coefficient (cm s^{-1}), A is the filter area (0.24 cm^2), V_A is the volume of the acceptor phase (0.3 ml), t is the incubation time (s), τ_{SS} is the time to reach the steady state (s), $c_A(t)$ is the concentration of the compound in the acceptor phase at time point t (mol mL^{-1}), and S (mol ml^{-1}) is the solubility of IND in the donor phase. The flux of samples was calculated using the following equation:

$$\text{Flux} = P_e \times S \quad (8)$$

2.11. Ex vivo semiquantitative tissue permeation study

Ex vivo permeability studies were performed on porcine small intestine obtained as a slaughterhouse by-product. Washing was performed via physiological saline solution. 1-centimeter-wide slices of the small intestine were used for the studies, from which the outer intestinal wall was removed and the intestinal epithelium layers were used (Sánchez et al., 2019). 50 μl of IND suspension and IND-PM dissolved formulation was dropped on the surface of the intestine, then 2 h incubation followed at 36.5°C. After the incubation, an incision was made on the dropping site and cross-sectional cuts were obtained with an average length of around 750 μm and width of 300 μm. These cross-sectional cuts were analysed via Raman spectroscopy and chemical mapping where the characteristic peaks of IND were profiled on the maps. The taken maps were 500 × 100 μm in lengths and widths. The measurement parameters were the same as explained before during the Raman study but with a step size of 50 μm.

2.12. Ex vivo quantitative permeability study

Ex vivo quantitative permeability studies were also performed on porcine small intestine with the same preparation method described above. After the removal of the outer intestinal wall, the intestine was placed between the donor and acceptor chambers of a modified Side-bi-Side® type modified horizontal diffusion cell to function as a membrane. Thus, passive diffusion was investigated at intestinal conditions, where the donor phases were 9.0 ml of IND suspension and IND-PM formulation dispersed in FaSSIF and FeSSIF solutions. The diffusion surface was 0.785 cm^2 allowed by the circle of the support element fixing the intestinal part in place. The acceptor phase was 9.0 ml of PBS (pH 7.4). At predetermined time points 50 μl of aliquots were taken from the acceptor chamber and the concentration was measured by HPLC. The taken aliquots were immediately replaced with 50 μl of PBS (pH 7.4). Flux (J), permeability coefficient (K_p) and apparent permeability (P_{app}) values were calculated by the following equations (Bartos et al., 2018):

$$J = \frac{m_t}{A \times t} \quad (9)$$

$$K_p = \frac{J}{C_d} \quad (10)$$

$$P_{app} = \frac{\Delta[C]_A \times V_A}{A \times C_d \times t} \quad (11)$$

where m_t is the permeated drug at t time, A is the surface of the membrane, C_d is the initial donor chamber concentration, $\Delta[C]_A$ is the concentration difference of IND in the acceptor compartment after 120 min and V_A is the volume of the acceptor chamber.

2.13. Cytotoxicity assay

Cytotoxic effect of the samples was determined *in vitro* using Caco-2 human colorectal adenocarcinoma cells by means of MTT ([3-(4,5-dimethylthiazol-2-yl)-2,5-diphenyltetrazolium bromide]) assay. Briefly, a limited number of the cells (5000/well) were seeded onto a 96-well microplate and became attached to the bottom of the well overnight (37°C, 5% carbon-dioxide tension). On the second day of the procedure, the test substances were added in serial dilutions (final concentrations were: 0.3, 1.0, 3.0, 10.0, 30.0, 100 μM IND). After an incubation period of 72 h, the living cells were assayed by the addition of 20 μl of 5 mg/mL MTT solution. After a 4 h incubation, the medium was removed and the precipitated formazan was dissolved in 100 μl/well of DMSO during a 30-min period of shaking. Finally, the reduced MTT was assayed at 545 nm, using a microplate reader. Untreated cells were taken as the negative control. Caco-2 cell line was purchased from the European Collection of Cell Cultures (Salisbury, UK) and cultured in Eagle's Minimum Essential Medium. All *in vitro* experiments were carried out on two 96-well dishes with at least five parallel wells. Student's unpaired t-test was used for statistical evaluation of the results obtained from the cell treated with IND or IND-PM (GraphPad Prism 5.01 software, GraphPad Software, San Diego, CA, USA).

3. Results and discussion

3.1. Characterization of IND-loaded spray dried polymeric micelles

3.1.1. Particle size and distribution analysis

The particle size and the related parameters were measured via laser diffraction method. It has been revealed that compared to the initial IND, the formulation has a smaller, reduced particle size. The average particle size (D[0.5]) was around 7.21 μm, and the decrease in Span indicates a narrowing of the size distribution curve. The measured parameters can be seen in Table 4.

3.1.2. Morphology

The morphology of the initial IND and the spray-dried formulation was analysed via scanning electron microscopy (SEM). In Fig. 1, it can be observed that the starting IND has an irregular particle shape in polydisperse size distribution. The shapes have an irregular edge structure independently of each other and the particles do not adhere to each other. In the case of the spray-dried particles, these irregularities cannot be observed, which can be explained by the encapsulation process inside the micellar core. It can be also due to the film-forming capability of SP and the drug amorphization process as explained below. The D-Tre particles have a nearly spheroidal morphology, on which the polymeric micelles forming components are sitting or they can be either in the core of these spheres. Some irregularities and adhered particles can be seen on the image, which can occur between the excess SP. These formations can affect the flowability of the powder, but when dispersed in water,

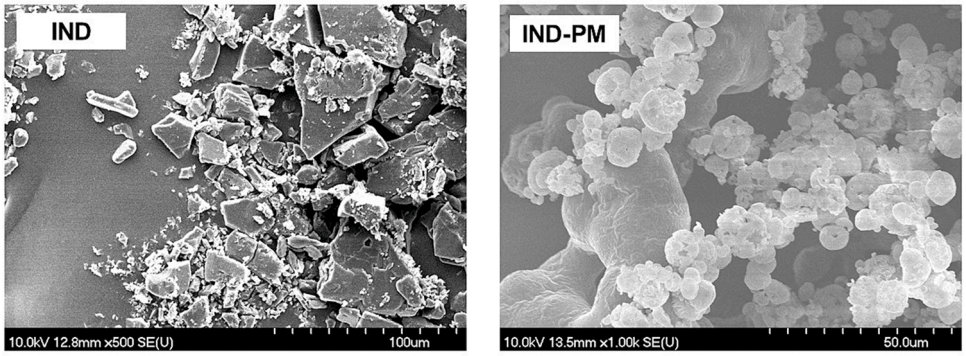

Fig. 1. Scanning electron microscopic images of initial IND and the spray-dried polymeric micelle formulation (IND-PM).

Table 5
Results from the stampfvolumetric measurement of the spray-dried particles compared to initial IND. Data are presented as means ± SD ($n = 3$).

	Bulk density (g/cm^3)	Tapped density (g/cm^3)	Hausner Ratio	Carr Index	Flowability
IND	1.316 ± 0.029	1.732 ± 0.037	1.316 ± 0.052	31.61 ± 2.02	poor
IND-PM	0.206 ± 0.013	0.239 ± 0.021	1.163 ± 0.039	16.02 ± 2.21	good

this would not cause any problem due to their quick hydration properties.

3.1.3. Density measurement

The spray-dried powder can be characterized with low density as it can be seen in Table 5. Based on the calculated Hausner Ratio and Carr Index, the flowability of the IND-PM formulation is good, compared with the initial IND.

3.1.4. Drug content

The drug content of the spray-dried polymeric micelle formulation was analysed via HPLC. After the dispersion in water, the amount of IND per gram was determined. This value was 1.242 ± 0.076% w/w, meaning that in 1000 mg of the formulation, there is 12.42 mg of IND in average. For further studies, 1000 mg of the spray-dried formulation was dispersed in 2 ml of purified water or the corresponding media, if not indicated otherwise.

3.1.5. Dynamic light scattering and zeta potential measurements

To characterize the polymeric micelles in aqueous media, dynamic light scattering and zeta potential measurement were applied to determine the micelle size, size distribution and surface charge properties. The measured average hydrodynamic particle size (expressed as Z-average) is 130 ± 2.3 nm, the polydispersity index is 0.241 ± 0.007 and the zeta potential is -12.3 ± 1.2 mV. All in all, it can be claimed that the polymeric micelles are in the nano size range in their characteristic size range in monodisperse distribution. This monodisperse distribution and the nano size range can offer uniform permeability along with increased water solubility and drug release. The surface charge of the particles is negative, meaning that the particles will repel each other which would indicate long term physical stability and the decrease in the tendency of aggregation in liquid state (Honary and Zahir, 2013).

3.1.6. Analysis on the increase in water solubility

To analyse the polymeric micelle formulation regarding the increase in water solubility, the encapsulation efficiency, the thermodynamic solubility was determined and wettability measurements were carried out. The thermodynamic solubility of IND and IND-PM was measured via the saturation method, where the filtrate's IND concentration was measured. In case of initial IND, the solubility was 0.778 ± 0.105 mg/ml, whilst the IND-PM formulation showed an increase to 18.431 ± 0.781 mg/ml which is almost a 24-fold increase in water solubility. This can be explained by the high micellization capacity of SP resulting in high encapsulation efficiency, which was 83.4 ± 1.8%. The wettability measurement (Table 6.) showed that the spray-dried formulation is wetted well with water, whilst initial IND is showing hydrophobic property. This is corroborated with the calculated polarity values: 23.24 and 41.70% for IND and IND-PM, respectively. The high polarity, proper wetting properties, the high encapsulation efficiency and increased solubility all can be explained by the decrease in particle size to the nano size range (Zhu et al., 2016). These results can also indicate rapid dissolution and efficient permeability across membranes which were investigated later.

3.2. Structure investigations

3.2.1. X-ray powder diffraction

Based on the obtained diffractograms (Fig. 2) from the XRPD investigation, it can be claimed that the spray-dried product is amorphous in nature. D-Tre is commonly used for stabilizing nanoparticles in case of spray or freeze-drying, and during this process, the characteristic peaks will disappear and the compound takes up an amorphous character as well (Sekitoh et al., 2021). In the formulation, the characteristic peaks of IND also do not show, which indicates that a new formulation was prepared where the IND is encapsulated in the micellar core. SP itself is also amorphous as the diffractogram of it shows.

3.2.2. Thermal analysis

Differential scanning calorimetry was performed to test the initial

Table 6
Contact angles against water and diiodomethane, surface free energy with the calculated percentage polarity values of the initial solid materials and the IND-PM formulation. Data are presented as means ± SD ($n = 3$).

Samples	Θ_{water} [°]	$\Theta_{diiodomethane}$ [°]	γ^d [mN m^{-1}]	γ^p [mN m^{-1}]	γ [mN m^{-1}]	Polarity (%)
IND	74.1 ± 4.9	13.1 ± 0.6	42.12	13.48	55.60	24.24
SP	33.4 ± 0.3	16.4 ± 0.0	44.02	29.20	73.22	39.88
D-Tre	18.7 ± 2.3	32.2 ± 2.1	41.49	32.13	73.62	43.64
IND-PM	28.1 ± 3.2	31.5 ± 3.1	44.90	32.11	77.01	41.70

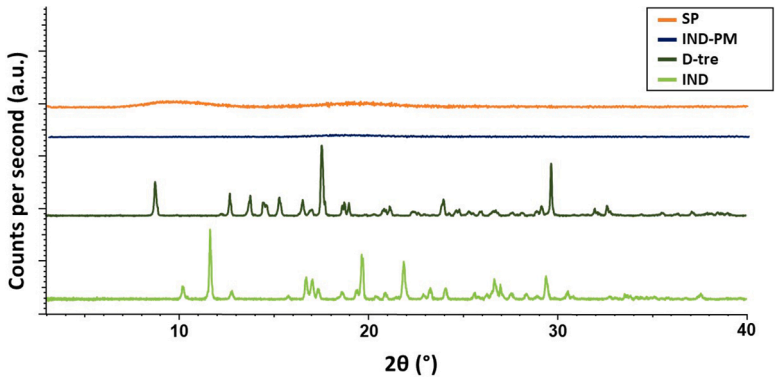

Fig. 2. X-ray powder diffractograms of the initial solid materials and the IND-PM spray-dried formulation.

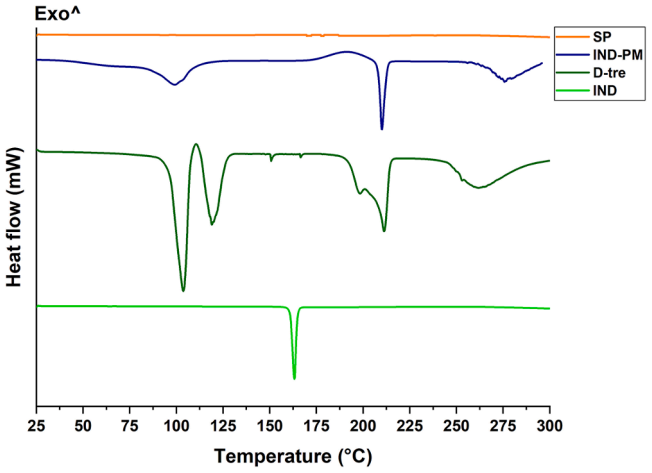

Fig. 3. DSC thermograms of the initial components and the IND-PM spray-dried formulation.

materials and the spray-dried product's thermal behaviour. It can be seen on Fig. 3, that the final product does not contain the characteristic endothermic peak of the initial IND (163.2°C) confirming successful encapsulation. On the thermogram of the IND-PM formulation, it can be seen that the characteristic melting points of D-Tre can be only found after the recrystallization around 189°C into anhydrous form, following it's immediately melting, indicating the endothermic peak at 210°C (Sekitoh et al., 2021). The polymeric micelle-forming polymer, SP, does not have an effect on the run down of the thermogram. As the formulation temperature was 110°C (inlet temperature), which is a lower value of the melting point of IND, it can be claimed that spray-drying is adequate for this procedure.

3.2.3. *Raman spectroscopy*

At first, Raman spectra of IND and the IND-PM formulation was taken, to investigate the effect of encapsulation to the structure of the

Table 7
Results of the physical stability investigation: dynamic light scattering (DLS) and laser diffraction measurements of the main particle- and nanoparticle characteristics. Abbreviations not used prior: ζ: zeta potential. Data are presented as means ± SD ($n = 3$).

Parameter	0 month	1 month	3 months	6 months
Z-average (nm)	130.0 ±7.4	132.3 ± 5.8	131.5 ± 6.9	134.6 ± 8.3
PdI	0.241 ±0.011	0.243 ±0.018	0.237 ± 0.019	0.242 ± 0.023
ζ (mV)	-12.3 ± 0.9	-11.9 ± 1.6	-12.3 ± 1.2	-12.4 ± 1.7
D [0.1] (μm)	2.33 ± 0.31	2.37 ± 0.17	2.41 ± 0.28	2.38 ± 0.22
D [0.5] (μm)	7.21 ± 0.34	7.31 ± 0.49	7.28 ± 0.37	7.33 ± 0.21
D [0.9] (μm)	15.23 ± 0.75	15.41 ± 0.39	15.37 ± 0.57	15.49 ± 0.46
Span	1.789 ± 0.097	1.784 ± 0.137	1.780 ± 0.069	1.788 ± 0.091

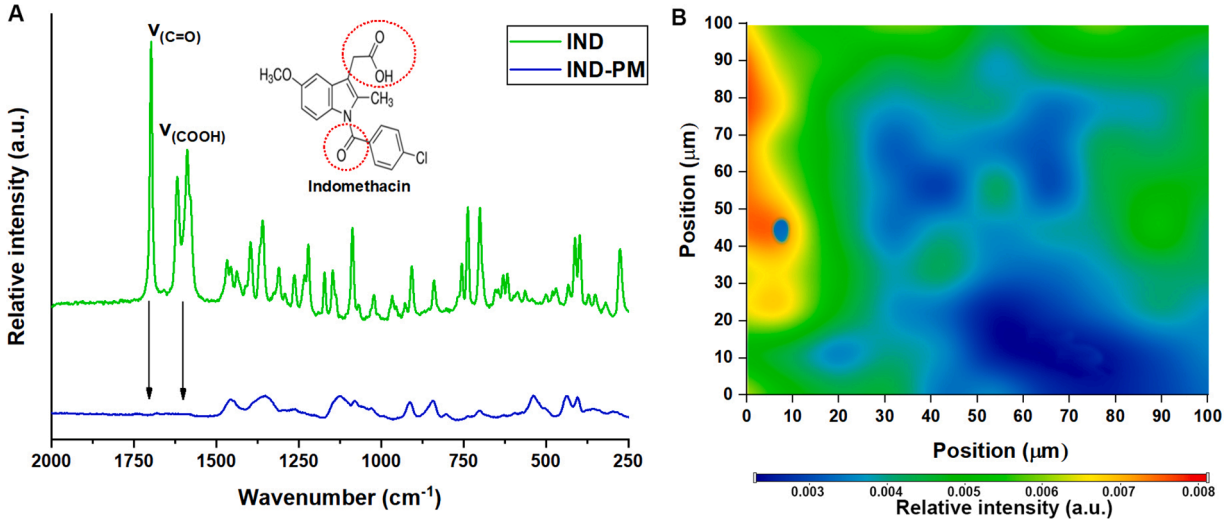

Fig. 4. (A) Raman spectra of initial IND and the IND-PM formulation highlighting the main difference in the characteristic peaks; (B) Raman chemical map of a pressed IND-PM formulation profiled with the distinguished characteristic peaks of IND.

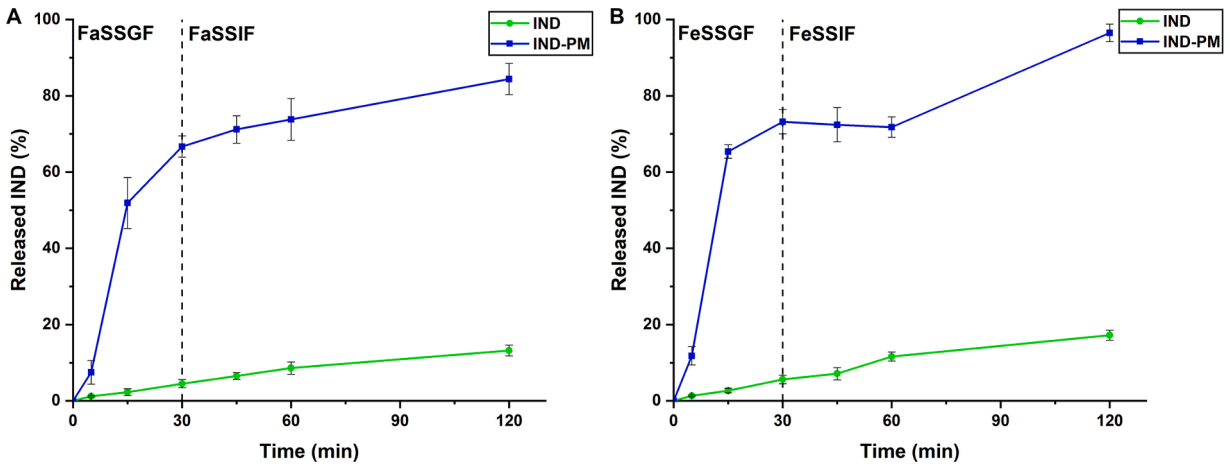

Fig. 5. *In vitro* drug release curves of data obtained at fasted state (A) and fed state (B) biorelevant dissolution media. Data are presented as means ± SD ($n = 3$).

Table 8
Obtained kinetic parameters of the spray-dried IND-loaded polymeric micelles compared to the initial IND. Abbreviations: Fa – fasted state conditions, Fe – fed state conditions.

Model		IND (Fa)	IND-PM (Fa)	IND (Fe)	IND-PM (Fe)
Zero order	k_0 (μg min^{-1})	0.1213	0.9718	0.1556	1.057
	R^2	0.9811	0.8051	0.9835	0.8024
	$t_{0.5}$ (min)	412.20	51.45	321.34	47.30
First order	k_1 (min^{-1}) x 10^{-3}	1.2	14.9	1.6	25.2
	R^2	0.9794	0.8233	0.9774	0.9091
	$t_{0.5}$ (min)	577.62	46.51	433.22	27.51
Second order	k_2 (μg^{-1} min^{-1}) x 10^{-5}	1.3	40	1.8	213.8
	R^2	0.9846	0.9760	0.9818	0.8120
	$t_{0.5}$ (min)	763.92	19.25	553	19.73
Korsmeyer-Peppas	$k_{K\text{-}P}$ (min^{-n}) x 10^{-3}	3.15	40.9	3.12	73.37
	n	0.7868	0.7211	0.8438	0.5934
	R^2	0.9910	0.7713	0.9878	0.7487
	$t_{0.5}$ (min)	218.30	19.11	96.08	59.56
Higuchi	k_H (μg $min^{-1/2}$)	1.058	9.298	1.3457	10.107
	R^2	0.9704	0.9572	0.9551	0.9529
	$t_{0.5}$ (min)	2231.72	28.92	1380.52	24.47
Hixon-Crowell	$k_{H\text{-}C}$ ($\mu g^{1/3}$ min^{-1}) x 10^{-3}	1.9	23.2	2.5	29.1
	R^2	0.9841	0.8659	0.9863	0.9105
	$t_{0.5}$ (min)	503.98	41.63	383.02	33.02
Best fit		Korsmeyer-Peppas	Second order	Korsmeyer-Peppas	Higuchi

IND. Two main characteristic absorptions were observed in the spectrum of initial IND at 1586 1/cm (ν_{COOH}) and 1697 1/cm ($\nu_{=O}$) (Fig. 4A). The Raman spectrum of the polymeric micelle showed that these peaks disappeared. This could be because of the hydrogen bonding amongst polymeric micelle forming components, which can enhance the intra-micelle interactions and micelle stability. These hydrogen bonding interactions are selective and noncovalent interactions. SP itself has a long backbone of PEG 6000 chain, which can form this hydrogen bonding with the carboxylic and the oxo group of the IND. Hydrogen bonding not only affects the stability of micelles, but it also directs the self-assembly behaviour of the co-polymer blocks and the drug loading in the micellar core (Sipos et al., 2020). On Fig. 4B, the Raman chemical map of a pressed IND-PM formulation can be seen, with the profile of the IND-specific peak region: 1520 to 1750 1/cm. The intensity scale shows really low values (0.003 to 0.008) which by itself indicates that these peaks are not presented in the formulation. Based on the map, it can be claimed that the API is distributed evenly through the pressed sample, and in the form of polymeric micelles, not as the initial API. This result is corroborated with the high encapsulation efficiency and the wettability measurements, where the outer hydrophilic micellar shell, along with the D-Tre enhanced the polarity of the formulation compared to initial IND.

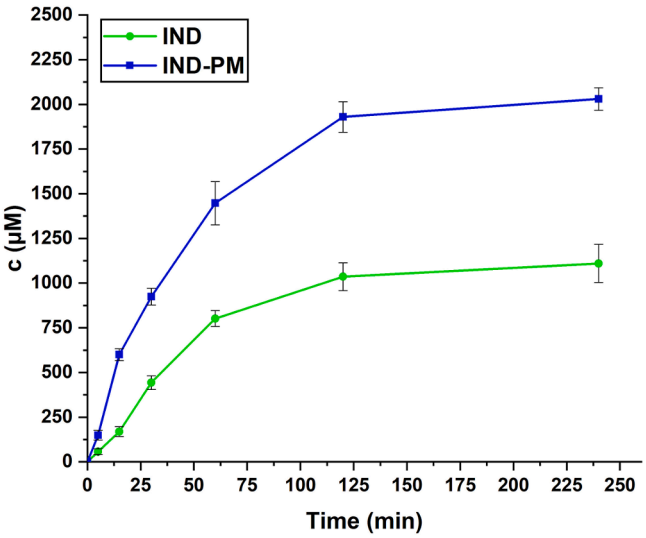

Fig. 6. Rapid equilibrium dialysis curves of IND (initial and IND-PM formulation). Results are expressed as means ± SD ($n = 5$).

3.3. Physical stability test

Conducting the intermediate stability test, it can be claimed that the formulation remained physically stable when stored in solid form. Based on the laser diffraction measurements, the main particle size characteristics remained the same with insignificant differences during the study. The stable particle size can be due to the good quality attributes of D-Tre and the Tween 80 is able to distinguish the spherical particles. The Span values all indicate a narrow size distribution as well. The DLS measurements revealed that the Z-average and PdI values also remained, which indicates that proper increase in water solubility, therefore advanced drug release and permeability can be achieved after

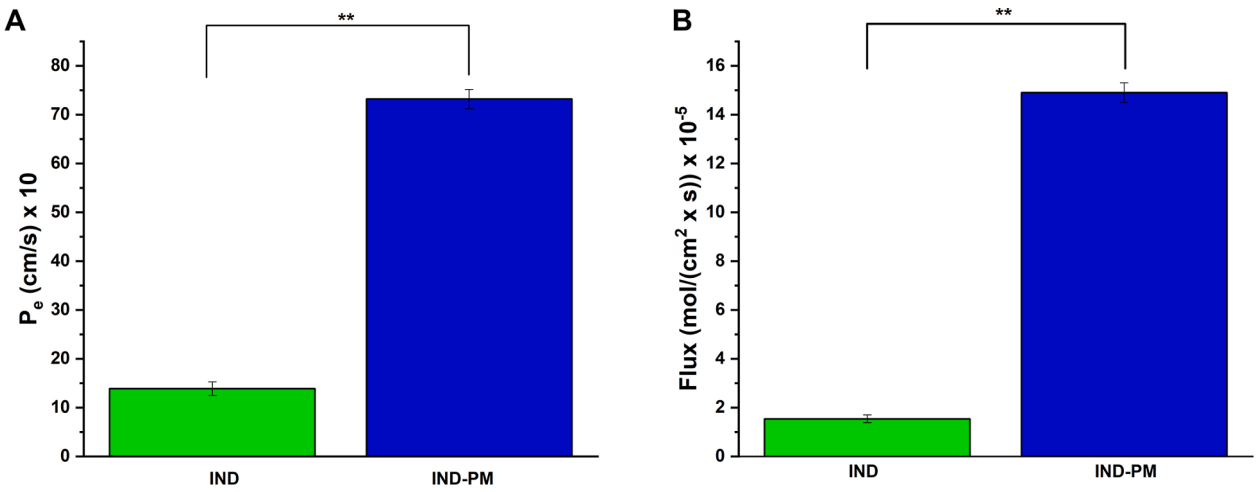

Fig. 7. Effective permeability (A) and flux (B) values of initial IND and the IND-PM formulation through the GI-PAMPA model. Data are presented as means ± SD (n = 6). ANOVA test was performed to check the significance between the measured samples. ** $p < 0.01$.

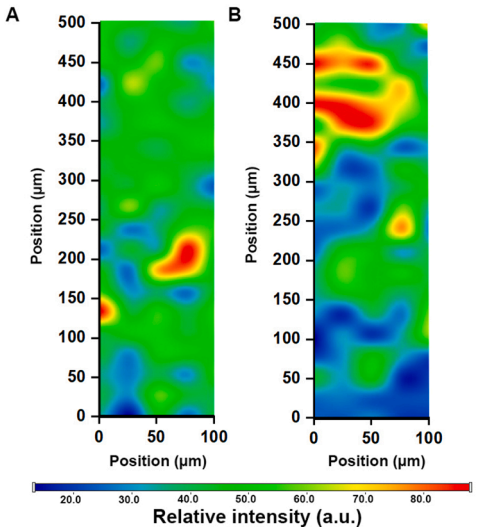

Fig. 8. Raman chemical maps of *ex vivo* semiquantitative tissue permeation study on porcine small intestine cuts. A: IND suspension, B: IND-PM spray-dried formulation

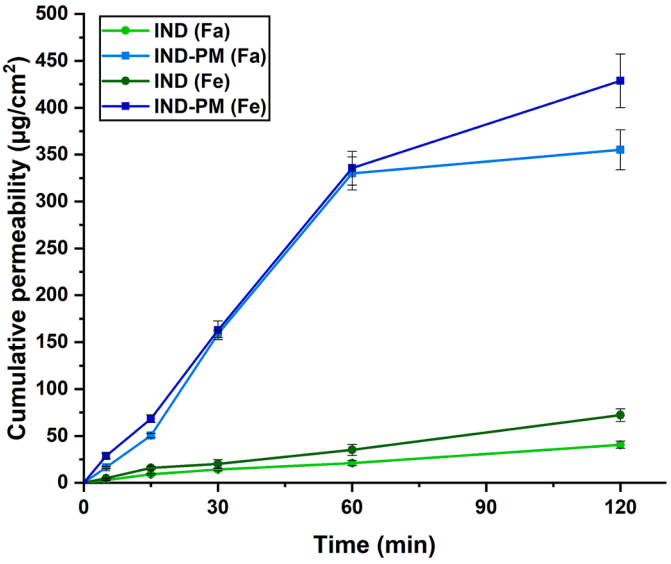

Fig. 9. *Ex vivo* cumulative permeability values of initial IND and IND-PM spray-dried formulations compared in fasted (Fa) and fed (Fe) state conditions. Data are presented as means ± SD (n = 3).

storage. No significant change in the zeta potential can be also found, which indicates that particle aggregation is unlikely due to the repelling forces between the negatively charged particles. The obtained results can be seen on Table 7.

3.4. *In vitro* drug release study

The maximum solubility of IND was determined prior in the micellar formulation (18.431 ± 0.781 mg/ml) and the maximum feasible concentration of releasable IND was 0.125 mg/ml, therefore sink conditions were highly respected. The *in vitro* dissolution study was performed with two different media (fasted and fed state gastric/intestinal fluids) with a gastrointestinal transfer protocol. The released IND was measured via HPLC, and expressed as a percentage of the stock solutions. The drug release curves can be seen on Fig. 5. It can be claimed that the polymeric micelle formulation showed higher drug release in both cases, compared to initial IND. This is due to several things: the nano size range, the increased water solubility and high encapsulation efficiency (Sethi et al., 2014). It can be also observed that higher percentage has been released during the simulated fed state studies. This indicates that if this product would be placed in market, the patient should take it after meals because it would lead to higher effective released drug concentration.

Table 9
Flux (J), permeability coefficient (K_p) and apparent permeability (P_{app}) values from the *ex vivo* permeability study compared in fasted (Fa) and fed (Fe) state conditions. Data are presented as means ± SD (n = 3).

Sample	J (μg/cm²)	K_p (cm/h)	P_{app} (cm/s) x 10^{-4}
IND (Fa)	40.60	1.461	1.299
IND-PM (Fa)	355.22	12.788	11.367
IND (Fe)	72.33	2.604	2.314
IND-PM (Fe)	428.69	15.433	13.718

Six different drug release kinetic profiles were fitted to the drug release curves, which calculated parameters can be seen on Table 8. As for the initial IND, the Korsmeyer-Peppas (R^2 = 0.9910 and 0.9878, respectively) fitting was the best in both fasted and fed state. In case of fasted state IND-PM drug release, the second order (R^2 = 0.9760) equation had the best fit and in the case of fed state IND-PM drug release,

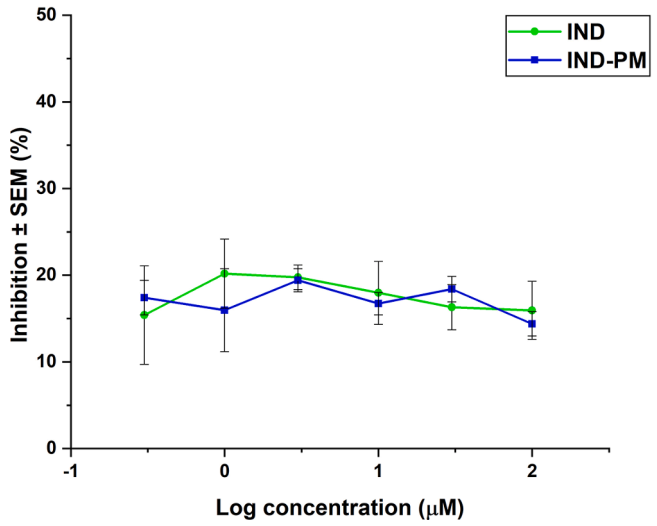

Fig. 10. Inhibition of viability of Caco-2 human colorectal adenocarcinoma cells treated IND suspension and the spray-dried IND-PM nanoformulation. Results are expressed as means ± SD ($n = 5$).

the Higuchi kinetic ($R^2 = 0.9529$) prevailed. This means that the release mechanism of IND from the polymeric micelle carrier is mainly controlled by the diffusion properties. This can be due to the fact, that polymeric micelles have high entropy, thus high motility in aqueous solutions, which will lead to diffusion-mediated drug release as well (Mehanny et al., 2016; Katona et al., 2022).

3.5. Rapid equilibrium dialysis assay

Rapid equilibrium dialysis (RED) assay was performed to investigate the equilibrium state kinetic of the IND-PM formulation. It was compared to initial IND suspension. Based on the RED curves (Fig. 6), similar run down can be experienced with initial IND, however at a significantly higher (IND-PM vs. IND, * $p < 0.05$) concentration levels. The equilibrium of the formulation stars to set after 2 h which is suitable for peroral administration as the average transit time of drugs in the small intestine is just around that time period. This also means that the formulation can achieve enhanced drug transport between the intestinal compartments.

3.6. PAMPA permeability assay

The PAMPA-Int permeability assay was performed to quantify the effective permeability and flux values across the artificial intestinal lipid barrier, as main predictor of characterizing the drug transport of the IND in the initial suspension and the IND-PM formulation (Fig. 7). Based on the measured and calculated data, it can be claimed that the IND-PM formulation showed significant increase in the P_e and flux values (IND-PM vs. IND, ** $p < 0.01$). This can be explained by the high encapsulation efficiency inside the penetration enhancer and solubilizer co-polymer (SP). These higher values also offer rapid onset of action due to the quick absorption to the bloodstream from the intestinal lumen. Although IND is a BCS Class II drug, meaning it has good intestinal permeability, it was also improved by the encapsulation process.

3.7. Ex vivo semiquantitative tissue permeation study

Ex vivo semiquantitative tissue permeation study was performed on porcine small intestine to determine the passive diffusion through the incised intestine section. The intestinal epithelium was investigated via Raman spectroscopy where the spectra of IND and IND-PM were profiled on the measured sections. Based on the Raman chemical maps on Fig. 8, it can be claimed that the IND-PM formulation diffused in deeper tissue regions compared to the initial IND suspension. It can also be observed that in the upper epithelial layers, the intensity values decreased immensely which means that faster accumulation in the deeper tissue layers would occur. Due to the decreased particle size and the diffusion-mediated drug release, the increased permeability was investigated quantitatively furthermore.

3.8. Ex vivo quantitative permeability study

The *ex vivo* quantitative permeability study was performed on porcine small intestine to determine the flux and permeability values during passive diffusion of initial IND and the IND-PM spray-dried formulation. The IND-PM formulation showed significant (IND-PM vs. IND, ** $p < 0.01$) increase in the cumulative permeability values compared to initial IND. This result can be experienced in both cases, where the donor chambers consisted of fasted or fed state intestinal fluids (Fig. 9). The calculated flux (J), permeability coefficient (K_p) and apparent permeability (P_{app}) values were also significantly increased compared to initial IND (Table 9.). The results can be explained by the fast drug release mechanism as measured before, alongside the decrease in the particle size and the penetration enhancer function of SP. The fed state measurement also showed higher values compared to the fasted state studies, which is similar to the *in vitro* drug release study.

3.9. Cytotoxicity assay

MTT assay was conducted in order to determine the cytotoxicity of the IND-PM formulation on Caco-2 human colorectal adenocarcinoma cell line. IND itself is safe to administer in the therapeutical dosage without relevant cytotoxic effect. The formulations were tested after the IND content was diluted to a range between 0.3 and 100 μM. As it can be seen on Fig. 10, no significant difference was experienced ($p > 0.05$) between the viabilities of the cell treated with reference IND suspension and the IND-PM polymeric micelle formulation.

4. Conclusion

In conclusion, a promising fast dispersible formulation was developed by spray-drying containing a value-added polymeric micelle formulation loaded with indomethacin intended for peroral administration as substitution possibility for conventional IND tablets. With the increased physical stability in solid form and the proper particle characteristics, *in vitro* and *ex vivo* studies, it can be confirmed that the polymeric micelle nanocarrier help with enhanced drug release, therefore intestinal permeability and holds the future to the further developed patient-centred and patient suited dosage systems.

Funding

The publication was funded by The University of Szeged Open Access Fund (FundRef, Grant No. 5653).

CRediT authorship contribution statement

Bence Sipos: Conceptualization, Methodology, Software, Formal analysis, Investigation, Data curation, Writing – original draft, Visualization, Project administration. **Ildikó Csóka:** Conceptualization, Methodology, Validation, Formal analysis, Resources, Writing – review & editing, Supervision, Project administration. **Rita Ambrus:** Software, Investigation, Writing – review & editing. **Zsuzsanna Schelz:** Software, Investigation, Writing – original draft. **István Zupkó:** Conceptualization, Validation, Resources, Writing – review & editing, Project administration. **György Tibor Balogh:** Resources, Investigation, Writing – original draft. **Gábor Katona:** Conceptualization, Methodology, Validation, Formal analysis, Resources, Writing – review & editing,

Supervision, Project administration.

Declaration of Competing Interest

The authors declare no conflict of interest.

Acknowledgements

This work was supported by the ÚNKP-21-3-SZTE-260 New National Excellence Program and by Project no. TKP2021-EGA-32 implemented with the support provided by the Ministry of Innovation and Technology of Hungary from the National Research, Development and Innovation Fund, financed under the TKP2021-EGA funding scheme.

References

Alvarez-Rivera, F., Fernández-Villanueva, D., Concheiro, A., Alvarez-Lorenzo, C., 2016. α-Lipoic acid in soluplus® polymeric nanomicelles for ocular treatment of diabetes-associated corneal diseases. J. Pharm. Sci. 105, 2855–2863. https://doi.org/10.1016/j.xphs.2016.03.006.

Avdeef, A., 2012. Permeability-PAMPA. Absorpt. Drug Dev. 319–498. https://doi.org/10.1016/j.ejps.2021.105960.

Badri, W., Miladi, K., Nazari, Q.A., Greige-Gerges, H., Fessi, H., Elaissari, A., 2016. Encapsulation of NSAIDs for inflammation management: overview, progress, challenges and prospects. Int. J. Pharm. 515, 757–773. https://doi.org/10.1016/j.ijpharm.2016.11.002.

Bartos, C., Pallagi, E., Szabó-Révész, P., Ambrus, R., Katona, G., Kiss, T., Rahimi, M., Csóka, I., 2018. Formulation of levodopa containing dry powder for nasal delivery applying the quality-by-design approach. Eur. J. Pharm. Sci. 123, 475–483. https://doi.org/10.1016/j.ejps.2018.07.061.

Baumann, J.M., Adam, M.S., Wood, J.D., 2021. Engineering advances in spray drying for pharmaceuticals. Annu. Rev. Chem. Biomol. Eng. 12, 217–240. https://doi.org/10.1146/annurev-chembioeng-091720-034106.

Bowey, K., Neufeld, R.J., 2010. Systemic and mucosal delivery of drugs within polymeric microparticles produced by spray drying. BioDrugs 24, 359–377. https://doi.org/10.2165/11539070-000000000-00000.

Deshmukh, A.S., Chauhan, P.N., Noolvi, M.N., Chaturvedi, K., Ganguly, K., Shukla, S.S., Nadagouda, M.N., Aminabhavi, T.M., 2017. Polymeric micelles: basic research to clinical practice. Int. J. Pharm. 532, 249–268. https://doi.org/10.1016/j.ijpharm.2017.09.005.

Eleraky, N.E., Swarnakar, N.K., Mohamed, D.F., Attia, M.A., Pauletti, G.M., 2020. Permeation-enhancing nanoparticle formulation to enable oral absorption of enoxaparin. AAPS PharmSciTech 21, 1–11. https://doi.org/10.1208/s12249-020-1618-2.

Eun, J.B., Maruf, A., Das, P.R., Nam, S.H., 2020. A review of encapsulation of carotenoids using spray drying and freeze drying. Crit. Rev. Food Sci. Nutr. 60, 3547–3572. https://doi.org/10.1080/10408398.2019.1698511.

Gaucher, G., Satturwar, P., Jones, M.C., Furtos, A., Leroux, J.C., 2010. Polymeric micelles for oral drug delivery. Eur. J. Pharm. Biopharm. 76, 147–158. https://doi.org/10.1016/j.ejpb.2010.06.007.

Gouda, R., Baishya, H., Qing, Z., 2017. Application of mathematical models in drug release kinetics of carbidopa and levodopa ER tablets. J. Dev. Drugs 06, 1–8. https://doi.org/10.4172/2329-6631.1000171.

Honary, S., Zahir, F., 2013. Effect of zeta potential on the properties of nano-drug delivery systems - a review (Part 1). Trop. J. Pharm. Res. 12, 255–264. https://doi.org/10.4314/tjpr.v12i2.19.

Stability Testing of New Drug Substances and Drug Products Q1A (R2), 2003. ICH, Geneva, Switzerland.

Irvine, J., Afrose, A., Islam, N., 2018. Formulation and delivery strategies of ibuprofen: challenges and opportunities. Drug Dev. Ind. Pharm. 44, 173–183. https://doi.org/10.1080/03639045.2017.1391838.

Katona, G., Sipos, B., Ambrus, R., Csóka, I., Szabó-Révész, P., 2022. Characterizing the drug-release enhancement effect of surfactants on megestrol-acetate-loaded granules. Pharmaceuticals 15. https://doi.org/10.3390/ph15020113.

Mehanny, M., Hathout, R.M., Geneidi, A.S., Mansour, S., 2016. Bisdemethoxycurcumin loaded polymeric mixed micelles as potential anti-cancer remedy: preparation, optimization and cytotoxic evaluation in a HepG-2 cell model. J. Mol. Liq. 214, 162–170. https://doi.org/10.1016/j.molliq.2015.12.007.

Mohammed, M., Mansell, H., Shoker, A., Wasan, K.M., Wasan, E.K., 2019. Development and *in vitro* characterization of chitosan-coated polymeric nanoparticles for oral delivery and sustained release of the immunosuppressant drug mycophenolate mofetil. Drug Dev. Ind. Pharm. 45, 76–87. https://doi.org/10.1080/03639045.2018.1518455.

Party, P., Bartos, C., Farkas, Á., Szabó-Révész, P., Ambrus, R., 2021. Formulation and *in vitro* and *in silico* characterization of "nano-in-micro" dry powder inhalers containing meloxicam. Pharmaceutics 13, 1–18. https://doi.org/10.3390/pharmaceutics13020211.

Radacsi, N., Giapis, K.P., Ovari, G., Szabó-Révész, P., Ambrus, R., 2019. Electrospun nanofiber-based niflumic acid capsules with superior physicochemical properties. J. Pharm. Biomed. Anal. 166, 371–378. https://doi.org/10.1016/j.jpba.2019.01.037.

Rahman, M., Coelho, A., Tarabokija, J., Ahmad, S., Radgman, K., Bilgili, E., 2020. Synergistic and antagonistic effects of various amphiphilic polymer combinations in enhancing griseofulvin release from ternary amorphous solid dispersions. Eur. J. Pharm. Sci. 150, 105354 https://doi.org/10.1016/j.ejps.2020.105354.

Ruphuy, G., Saloň, I., Tomas, J., Šalamúnová, P., Hanuš, J., Štěpánek, F., 2020. Encapsulation of poorly soluble drugs in yeast glucan particles by spray drying improves dispersion and dissolution properties. Int. J. Pharm. 576 https://doi.org/10.1016/j.ijpharm.2019.118990.

Sánchez, A.B., Calpena, A.C., Mallandrich, M., Clares, B., 2019. Validation of an *ex vivo* permeation method for the intestinal permeability of different BCS drugs and its correlation with Caco-2 *in vitro* experiments. Pharmaceutics 11, 1–12. https://doi.org/10.3390/pharmaceutics11120638.

Sekitoh, T., Okamoto, T., Fujioka, A., Yoshioka, T., Terui, S., Imanaka, H., Ishida, N., Imamura, K., 2021. Crystallization characteristics of amorphous trehalose dried from alcohol. J. Food Eng. 292, 110325 https://doi.org/10.1016/j.jfoodeng.2020.110325.

Sethi, M., Sukumar, R., Karve, S., Werner, M.E., Wang, E.C., Moore, D.T., Kowalczyk, S. R., Zhang, L., Wang, A.Z., 2014. Effect of drug release kinetics on nanoparticle therapeutic efficacy and toxicity. Nanoscale 6, 2321–2327. https://doi.org/10.1039/c3nr05961h.

Simões, S.M.N., Figueiras, A.R., Veiga, F., Concheiro, A., Alvarez-Lorenzo, C., 2015. Polymeric micelles for oral drug administration enabling locoregional and systemic treatments. Expert Opin. Drug Deliv. 12, 297–318. https://doi.org/10.1517/17425247.2015.960841.

Sipos, B., Csóka, I., Budai-Szűcs, M., Kozma, G., Berkesi, D., Kónya, Z., Balogh, G.T., Katona, G., 2021. Development of dexamethasone-loaded mixed polymeric micelles for nasal delivery. Eur. J. Pharm. Sci. 166 https://doi.org/10.1016/j.ejps.2021.105960.

Sipos, B., Szabó-Révész, P., Csóka, I., Pallagi, E., Dobó, D.G., Bélteky, P., Kónya, Z., Deák, Á., Janovák, L., Katona, G., 2020. Quality by design based formulation study of meloxicam-loaded polymeric micelles for intranasal administration. Pharmaceutics 12, 1–29. https://doi.org/10.3390/pharmaceutics12080697.

Uhljar, L.É., Kan, S.Y., Radacsi, N., Koutsos, V., Szabó-Révész, P., Ambrus, R., 2021. *In vitro* drug release, permeability, and structural test of ciprofloxacin-loaded nanofibers. Pharmaceutics 13, 1–18. https://doi.org/10.3390/pharmaceutics13040556.

Wang, Q., Fotaki, N., Mao, Y., 2009. Biorelevant dissolution: Methodology and application in drug development. Dissolut. Technol. 16, 6–12. https://doi.org/10.14227/DT160309P6.

Wijiani, N., Isadiartuti, D., Agus Syamsur Rijal, M., Yusuf, H., 2020. Characterization and dissolution study of micellar curcumin-spray dried powder for oral delivery. Int. J. Nanomed. 15, 1787–1796. https://doi.org/10.2147/IJN.S245050.

Wójcik-Pastuszka, D., Krzak, J., Macikowski, B., Berkowski, R., Osiński, B., Musiał, W., 2019. Evaluation of the release kinetics of a pharmacologically active substance from model intra-articular implants replacing the cruciate ligaments of the knee. Materials 12. https://doi.org/10.3390/ma12081202. Basel.

Xia, D., Yu, H., Tao, J., Zeng, J., Zhu, Q., Zhu, C., Gan, Y., 2016. Supersaturated polymeric micelles for oral cyclosporine a delivery: the role of Soluplus-sodium dodecyl sulfate complex. Colloids Surf. B Biointerfaces 141, 301–310. https://doi.org/10.1016/j.colsurfb.2016.01.047.

Yan, Y.D., Kim, J.A., Kwak, M.K., Yoo, B.K., Yong, C.S., Choi, H.G., 2011. Enhanced oral bioavailability of curcumin via a solid lipid-based self-emulsifying drug delivery system using a spray-drying technique. Biol. Pharm. Bull. 34, 1179–1186. https://doi.org/10.1248/bpb.34.1179.

Yokoyama, M., 2010. Polymeric micelles as a new drug carrier system and their required considerations for clinical trials. Expert Opin. Drug Deliv. 7, 145–158. https://doi.org/10.1517/17425240903436479.

Zhu, J., Ou, X., Su, J., Li, J., 2016. The impacts of surface polarity on the solubility of nanoparticle. J. Chem. Phys. 145 https://doi.org/10.1063/1.4959805.